

WHERE ARE THE MINI KREUTZ-FAMILY COMETS?

QUAN-ZHI YE (叶泉志)¹, MAN-TO HUI (许文韬)², RAINER KRACHT³, AND PAUL A. WIEGERT¹

¹ Department of Physics and Astronomy, The University of Western Ontario, London, Ontario N6A 3K7, Canada; qye22@uwo.ca

² Department of Earth, Planetary and Space Sciences, University of California at Los Angeles,

595 Charles Young Drive East, Los Angeles, CA 90095-1567, USA

³ Ostlandring 53, D-25335 Elmshorn, Schleswig-Holstein, Germany

Received 2014 August 13; accepted 2014 September 30; published 2014 November 10

ABSTRACT

The Kreutz family of sungrazing comets contains over 2000 known members, many of which are believed to be under ~ 100 m sizes (*mini comets*) and have only been studied at small heliocentric distances (r_H) with space-based *SOHO/STEREO* spacecraft. To understand the brightening process of mini Kreutz comets, we conducted a survey using CFHT/MegaCam at moderate r_H guided by *SOHO/STEREO* observations. We identify two comets that should be in our search area but are not detected, indicating that the comets have either followed a steeper brightening rate within the previously reported rapid brightening stage (the *brightening burst*), or the brightening burst starts earlier than expected. We present a composite analysis of the pre-perihelion light curves of five Kreutz comets that cover to ~ 1 AU. We observe significant diversity in the light curves that can be used to grossly classify them into two types: C/Ikeya-Seki and C/SWAN follow the canonical r_H^{-4} while the others follow r_H^{-7} . In particular, C/SWAN seems to have undergone an outburst ($\Delta m > 5$ mag) or a rapid brightening ($n \gtrsim 11$) between $r_H = 1.06$ AU and 0.52 AU, and shows hints of structural/compositional differences compared to other bright Kreutz comets. We also find evidence that the Kreutz comets as a population lose their mass less efficiently than the dynamically new comet, C/ISON, and are relatively devoid of species that drive C/ISON's activity at large r_H . Concurrent observations of C/*STEREO* in different wavelengths also suggest that a blueward species such as CN may be the main driver for brightening bursts, instead of sodium as previously thought.

Key words: comets: general – comets: individual (C/1965 S1 (Ikeya-Seki), C/2011 W3 (Lovejoy), C/2012 E2 (SWAN), C/2012 S1 (ISON), C/2012 U3 (*STEREO*), SOHO-2388)

Online-only material: color figures

1. INTRODUCTION

First identified by Kreutz (1888), the Kreutz family of sungrazing comets is probably the most well-known comet family, mostly because of its small perihelion distance (almost at the surface of the Sun) and the large number of known members (~ 2000 as of the time of writing). Some of the most spectacular comets in history also belong to the Kreutz family, such as the Great Comet of 1843 (C/1843 D1 or 1843 I), the Great Comet of 1882 (C/1882 R1 or 1882 II), and Comet Ikeya-Seki in 1965 (C/1965 S1 or 1965f). However, until a few decades ago, the investigation of the Kreutz family had been restricted to the few brightest members, mostly because of the very unfavorable visibility for ground-based observers due to the extreme orbit geometry; most members are too faint and too close to the Sun to be observed from the ground.

Space-based solar coronagraphs launched in the 1970s and 1980s have proved to be good comet observatories as well (e.g., MacQueen & St. Cyr 1991, and many others), as they can detect sungrazing comets very close to the Sun. The *Solar and Heliospheric Observatory (SOHO)*, launched into a “halo orbit” near Earth's L1 point in 1995 (Domingo et al. 1995), is still operational and has found ~ 2800 comets as of 2014 September, most of which are Kreutz family members with sizes believed to be under ~ 100 m (for convenience, we term such objects *mini comets* without any physical implication). Mini comets are essentially transitional objects from comets to meteoroids, they are direct products in cometary fragmentation and form the base of the Kreutz hierarchy. While the success of *SOHO* has allowed us to look into some general questions about the Kreutz family

such as the dynamical evolution of the hierarchy (e.g., Sekanina & Chodas 2004, 2007; Sekanina & Kracht 2013), further studies are limited by short observation arcs (within a few days of the perihelia), low astrometric precision, and relatively high image noise of *SOHO*.

Ground-based observations of mini Kreutz comets, on the other hand, remains difficult and no successful observations have been reported. The only reported attempt was made by Knight et al. (2010, hereafter K10), who used the 4 m KPNO telescope and the 6.5 m Magellan telescope at Las Campanas to search for Kreutz comets 3–6 months prior to their expected arrivals at perihelia, with no positive detection reported. Robert McNaught (2007, private communication) also conducted similar searches at comparable elongations, with the 0.5 m Uppsala telescope at Siding Spring Observatory, but also did not find any comet.

One of the top questions involves the brightening process of these comets, which may bear implications about the structure and composition of the comets (e.g., Kimura et al. 2002). K10's analysis of some 1000 Kreutz comets observed by *SOHO* shows a stage of rapid brightening following $n \sim 7$ from an unknown heliocentric distance r_H (K10 noted that it is “unlikely” to be beyond $50 R_\odot$) to $\sim 24 R_\odot$, where n is defined such that the comet brightens following r_H^{-n} where r_H is the heliocentric distance. For convenience of discussion, we call this feature the *brightening burst*. It is unclear how far the brightening burst extends, but understanding this behavior would give clues about the volatile content and compositional diversity within the Kreutz family.

For this paper, we conducted a search for mini Kreutz comets at moderate heliocentric distance (~ 1 AU) to explore

Table 1
SOHO/STEREO Instruments Used for Kreutz Comet Observations,
 Compiled from Eyles et al. (2009) and Knight et al. (2010)

Spacecraft	Instrument	Bandpass	Resolution	Field of View
<i>SOHO</i>	Coronagraph 2 (C2)	400–850 nm	12'' pixel ⁻¹	2–6 R_{\odot}
<i>SOHO</i>	Coronagraph 3 (C3)	400–850 nm	56'' pixel ⁻¹	4–30 R_{\odot}
<i>STEREO</i>	Coronagraph 2 (COR-2)	650–750 nm	15'' pixel ⁻¹	2–15 R_{\odot}
<i>STEREO</i>	Heliospheric Imager 1 (HI-1)	630–730 nm ^a	70'' pixel ^{-1b}	3°–23° along ecliptic

Notes.

^a Some transmission at 370–420 nm and 930–950 nm (Bewsher et al. 2010).

^b The pixel size of the detector is 35'' pixel⁻¹, but the observations we used are binned by a factor of two.

the brightening behavior of these comets. This was done by surveying the “sweet spots” defined through the Kreutz Population Model (Sections 2 and 3), appropriate to comets ~ 1 AU from the Sun. The results are then combined with the observations from space-based coronagraphs (such as *SOHO*) to produce composite light curves (Section 4). The results are discussed and compared to several bright historical Kreutz comets observed at moderate r_H (Section 5).

2. METHODOLOGY

The century-old method of comet searching is to scan the regions that are statistically most likely to contain comets. This does not require a priori knowledge of the position of individual comets. However, for the case of Kreutz comets, there are two issues: (a) the dynamical evolution of the Kreutz family is quite complicated and many details are not clear (e.g., Marsden 1967, 1989; Sekanina & Chodas 2004; Sekanina & Kracht 2013), and (b) the orbital elements of almost all currently known Kreutz comets are derived from low-resolution *SOHO* observations, which results in large uncertainties. The two issues cause large uncertainties in the on-sky positions of the Kreutz comets at moderate r_H , on the order of several tens of square degrees at 1 AU.

Additionally, we can now make use of the new *Solar Terrestrial Relations Observatory (STEREO)* spacecraft that provides rather a long baseline when coupled with *SOHO* observations to help comet orbit determination (Table 1). *STEREO* consists of two identical satellites that orbit the Sun on about the same orbit of the Earth, but one is leading the Earth (*STEREO-A*) and the other is trailing the Earth (*STEREO-B*). The most useful instrument for improving the orbit determination is perhaps COR-2, an instrument on board *STEREO* that comes with high resolution and a large field-of-view, but is insensitive to faint comets due to its observing bandpass.

For the case of searching for mini Kreutz comets, one needs to cover a large area (at the order of 10 deg²) with deep limiting magnitude ($\gtrsim 20$ mag). Since earlier studies have suggested that Kreutz comets may have a steep brightening rate that makes detection far beyond Earth’s orbit exceedingly difficult, one also needs to search at the smallest elongation possible. Last, the search zones for Kreutz comets are located in the southern skies, which severely limits the use of northerly facilities.

3. KREUTZ POPULATION MODEL

To determine our surveying areas, we consider the distribution of orbital elements of 1253 known Kreutz comets, most of which were discovered in 1996–2008 by *SOHO* (Figure 1).⁴

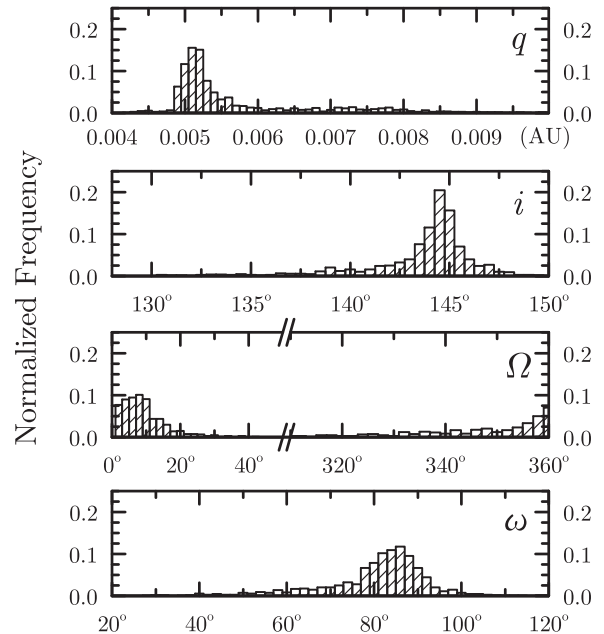


Figure 1. Distribution of orbital elements (perihelion distance q , inclination i , longitude of the ascending node Ω , and argument of perihelion ω) from 1 283 Kreutz comets selected from JPL small-body database.

The orbital elements are obtained from the JPL small-body database.⁵ According to this distribution of orbital elements, we then generate 10,000 pseudo comets 30 ± 15 days ahead of their perihelion passages and centered at our desired observing time. We also assign an absolute magnitude for each pseudo comet following K10’s size distribution, assuming geometric albedo $A_p = 0.05$, which allows us to calculate the apparent magnitude of the comet using K10’s “worst case” scenario: comets follow $n = 4$ until $50 R_{\odot}$, then follow $n = 7$ until $24 R_{\odot}$, where they move back $n = 4$ and remain so until reaching the average distance of peak brightness at $12 R_{\odot}$. We find the median brightness at $\Delta = r_H = 1$ AU (Δ is the geocentric distance) is about 21 mag. Depending on the season, the median motion of the pseudo comets varies from a few arc seconds per minute to 10–20 arcsec per minute.

We recognize the weakness of randomly distributing each orbital element as this assumes that each element is independent from each other. However, it has been known that the Kreutz family is composed by at least two (probably more) sub-groups, and the abundance and spread of each sub-group is not clearly known. We think that the current model is practically the best approach at the moment, which, when coupled with a “worst

⁴ Many post-2008 comets do not have published orbits at the time of study.

⁵ http://ssd.jpl.nasa.gov/sbdb_query.cgi, retrieved 2012 August 17.

Table 2
Details of the CFHT Observations

Date	R.A. Range	Decl. Range	Elongation	FWHM	1σ Efficiency in g'
2012 Sep 19	08 ^h 40 ^m to 08 ^h 48 ^m	−10° to −7°	~46°	~1''0	21.0
2012 Sep 20	08 ^h 36 ^m to 08 ^h 44 ^m	−10° to −7°	~48°	~1''5	21.0
2012 Sep 22	08 ^h 36 ^m to 08 ^h 44 ^m	−11° to −8°	~49°	~1''1	22.0
2012 Oct 16	10 ^h 11 ^m to 10 ^h 17 ^m	−20° to −14°	~47°	~2''0	22.0
2012 Oct 17	10 ^h 11 ^m to 10 ^h 17 ^m	−22° to −16°	~48°	~1''7	22.0
2012 Oct 18	10 ^h 11 ^m to 10 ^h 17 ^m	−22° to −16°	~49°	~1''4	22.0
2012 Oct 20	10 ^h 19 ^m to 10 ^h 25 ^m	−22° to −16°	~49°	~1''4	21.5
2012 Oct 21	08 ^h 19 ^m to 10 ^h 25 ^m	−23° to −17°	~50°	~1''2	22.0

Notes. The 1σ detection efficiency is determined based on the completeness of detection of artificial moving sources implanted in the actual data (see main text).

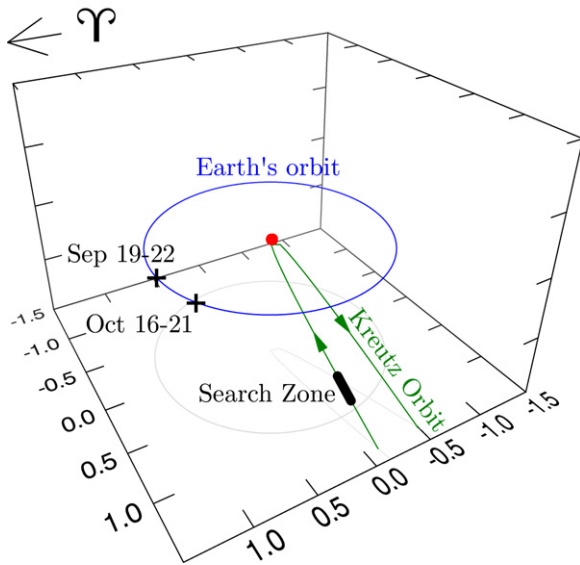


Figure 2. Observation circumstances and the search zone showed in a heliocentric frame. The arrow at the top left corner points to the Vernal Equinox (Υ). The two plus signs indicate the position of the Earth at the time of observation. The units of the axes are in AU. The cometary orbital plane is below the ecliptic plane. The size of the Sun is not to scale.

(A color version of this figure is available in the online journal.)

scenario” brightening model, should give us an idea about the lower limits of on-sky comet densities.

4. OBSERVATION AND ANALYSIS

4.1. CFHT Observation and Initial Analysis

We used the 3.6 m Canada–France–Hawaii Telescope (CFHT) with the 1 deg² MegaCam for our survey. A northerly latitude (19.8° N) prohibits observation when the Earth is closest to the common orbit of the Kreutz comets (which occurs in late December and solely favors southern hemisphere observers), but observation is still feasible in September and October, when the Earth is at moderate distance (~ 1 AU) to the inbound leg of the Kreutz comets (Figure 2). At 25° elevation and with a seeing of 1''5, we expected to reach $m_g = 23$ mag with 30 s exposures. Although bandpasses at longer wavelengths such as r' are slightly less responsive to atmospheric extinction, we chose g' as it includes most of the optical emission species (mostly C₂ and C₃ species) that may increase the chance of detection. We took three 30 s exposures at each position, separated by ~ 5 minutes to distinguish moving objects. To maximize the overall coverage, we did not make attempts to fill the gaps be-

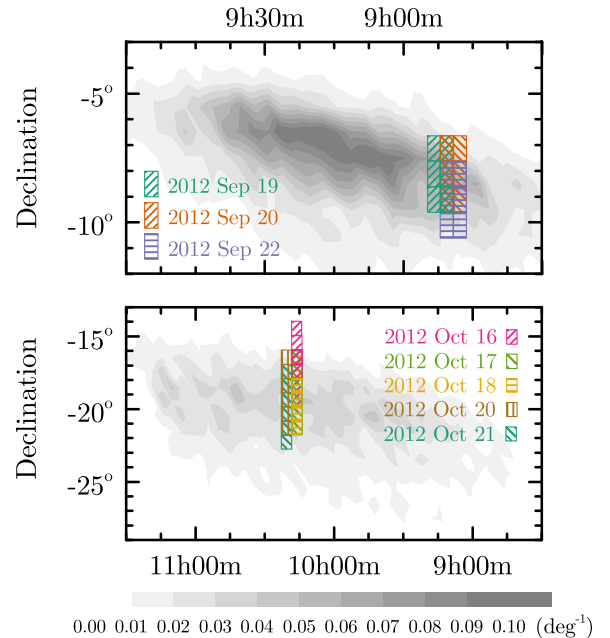


Figure 3. Simulated density of comets on 2012 September 20 and October 20, as well as the observed areas.

(A color version of this figure is available in the online journal.)

tween individual CCDs, hence the filling factor at each pointing location is 93% (de Kat & Abbon 2000).

We ran the Kreutz Population Model targeting for 2012 September 20 and 2012 October 20 for pseudo-comets that would reach their perihelia between 2012 October 5 to 2012 December 5. Considering the arrival rate of comets visible to C3 (i.e., peak brightness < 8 mag) in this season is ~ 10 per month as noted by K10, we find a maximum density of 0.04–0.08 comets per square degree. We note that the actual density in the “sweet spots” should be higher if the orbital elements are dependent on each other. The observations were executed around the two dates, as summarized in Table 2. The observed areas are shown in Figure 3.

After standard calibration (i.e., bias/dark field subtraction and flat-field division), the images are processed by a series of semi-automatic routines that looked for moving sources as developed by Wiegert et al. (2007), Gilbert & Wiegert (2009, 2010), and August & Wiegert (2013). Automatic detections are manually verified to remove false positives. No possible Kreutz comets were found in the data.

To determine the detection efficiency, we seed artificial sources that mimic brightness and movement of possible Kreutz

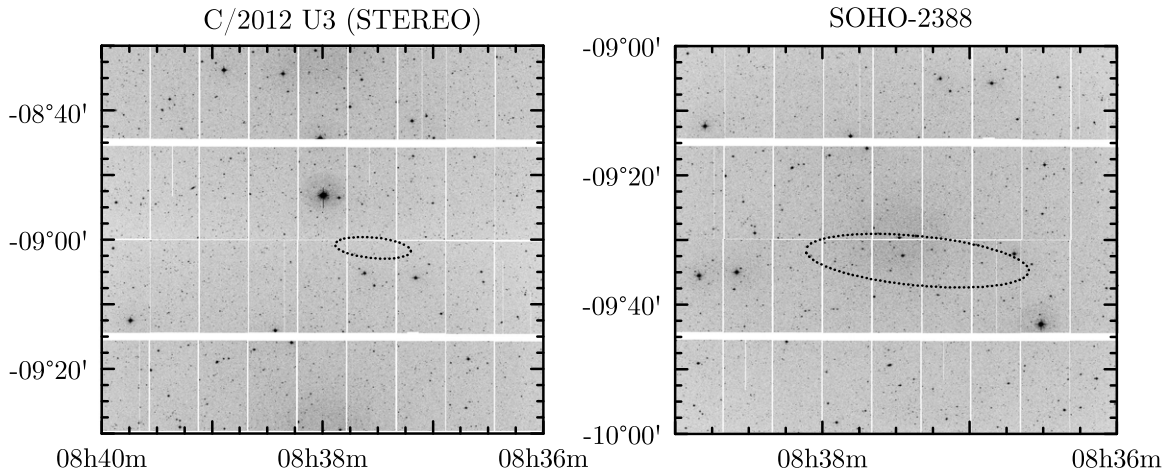


Figure 4. On-sky uncertainties of C/2012 U3 (*STEREO*) (left) and *SOHO*-2388 (right) on real CFHT observations on 2012 September 20 (C/*STEREO*) and September 22 (*SOHO*-2388).

Table 3
Kreutz Comets with *STEREO*-derived Orbits That are Searched
Against the CFHT Observations

Comet	Data Date	Detection Limit ^a	Comments
<i>SOHO</i> -2374	2012 Sep 19–22	...	Too far east
<i>SOHO</i> -2375	2012 Sep 19–22	...	Too far east
C/2012 U3 (<i>STEREO</i>)	2012 Sep 20	23.7 g ^r	Within FoV
<i>SOHO</i> -2388	2012 Sep 22	24.0 g ^r	Within FoV
<i>SOHO</i> -2404	2012 Oct 16–21	...	10° too west

Note. ^a Computed at $S/N = 3$ at the star masked combined data.

comets into one arbitrarily chosen data set from each night. The seeded images are processed by the same routines used for real data. The magnitudes of detected artificial sources are binned into 0.5 mag to determine completeness of detection along magnitude ranges. The lower boundaries of magnitude bins above 1σ detection efficiency are reported in Table 2.

4.2. Combined Analysis with *SOHO/STEREO* Data

After the expected perihelion passages of possible Kreutz comets that should be in our images, we check comets detected by *SOHO/STEREO* to see if there is any comet with an orbit accurate enough to pinpoint its position in our images. *SOHO* found 36 Kreutz comets in the time window set up for simulation (2012 October 5 to 2012 December 5), but due to the large on-sky uncertainties of *SOHO*-based Kreutz comets, we focus on the comets that are concurrently detected in COR-2. We identify five such comets (Table 3), but none of these five comets are published;⁶ therefore, we need to compute their orbits first. We obtain the raw “level-0.5” data from the *STEREO* public database, and calibrate them using the SolarSoft IDL package (Freeland & Handy 1998). We then perform astrometric measurements using the NOMAD catalog (Zacharias et al. 2004) and calculate their orbits using the EXORB program⁷ (Table 4). The uncertainties of the orbital elements are computed

⁶ One comet, temporarily sequenced as *SOHO*-2387, was published later using our reported measurements and received an official designation as C/2012 U3 (*STEREO*); the comet was first detected in *SOHO* data despite being named after *STEREO*. We will stick to the official designation C/2012 U3 (*STEREO*) in this study, but use unofficial *SOHO* sequence numbers for unpublished comets.

⁷ <http://chemistry.unina.it/~alvitagl/solex/Exorb.html>, retrieved 2014 July 21.

Table 4
Orbits of the Kreutz Comets That are Searched in CFHT Observations as
Derived Using *STEREO* Observations

Designation	T_p (UT)	q	e	i	ω	Ω
<i>SOHO</i> -2374	2012 Oct 6.86	0.0054	1.0	143°98	81°83	3°12
<i>SOHO</i> -2375	2012 Oct 13.80	0.0049	1.0	144°05	80°55	1°42
C/2012 U3 (<i>STEREO</i>)	2012 Oct 31.33	0.0053	1.0	144°14	81°18	1°45
<i>SOHO</i> -2388	2012 Nov 4.84	0.0046	1.0	144°22	80°47	0°32
<i>SOHO</i> -2404	2012 Nov 27.40	0.0047	1.0	144°13	80°55	0°94

using a Monte Carlo subroutine within EXORB, which allow us to estimate the on-sky uncertainty of the comet.

Two comets, C/*STEREO* and the unpublished *SOHO*-2388, are found to be within the field of view of images taken in 2012 September 20 and 22 (Figure 4). We mask out background stars and stack the images at the calculated motions of the comets to pull the limits, but still do not find any comets. The detection limits (assuming $S/N = 3$) of the stacked images are $m_g^r = 23.7$ for C/*STEREO* and $m_g^r = 24.0$ for *SOHO*-2388. We convert the magnitudes to Johnson V magnitude using the using CFHT transformation equations,⁸ and Jordi et al. (2006) assuming solar colors, which gives $m_V = 22.3$ and $m_V = 22.5$ normalized to $\Delta = r_H = 1$ AU.

We also measure the light curves of C/*STEREO* and *SOHO*-2388 in *SOHO/STEREO* data. The reduction procedure follows K10 for *SOHO* data and Hui (2013) for *STEREO* data, including normalization to $\Delta = 1$ AU and the phase angle $\theta = 90^\circ$ following the compound Henyey–Greenstein model (Marcus 2007):

$$\phi(\theta) = \frac{\delta_{90}}{1 + \delta_{90}} \left\{ k \left[\frac{1 + g_f^2}{1 + g_f^2 - 2g_f \cos(\pi - \theta)} \right]^{\frac{3}{2}} + (1 - k) \left[\frac{1 + g_b^2}{1 + g_b^2 - 2g_b \cos(\pi - \theta)} \right]^{\frac{3}{2}} + \frac{1}{\delta_{90}} \right\}, \quad (1)$$

where $\phi(\theta)$ is the scattering function that relates to magnitude by $m(\theta) = 2.5 \log \phi(\theta)$, δ_{90} is the dust-to-gas flux ratio at $\theta = 90^\circ$, k is the partitioning coefficient between forward and

⁸ <http://www2.cadc-ccda.hia-ihp.nrc-cnrc.gc.ca/en/megapipe/docs/filt.html> retrieved 2014 July 21.

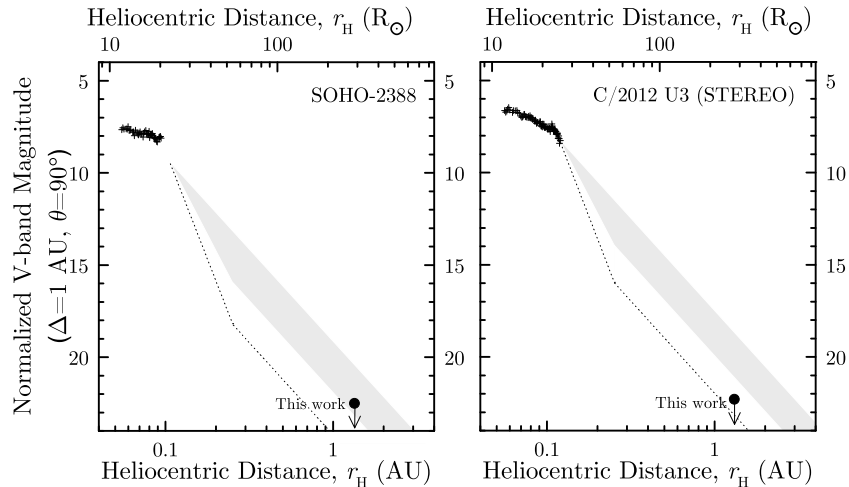


Figure 5. light curve of C/2012 U3 (*STEREO*) (left) and *SOHO*-2388 (right) using C3 data, as well as the upper limits constrained by CFHT observations. The shaded area is the set of possible light curves from no brightening burst ($n = 4$) to nominal rate of brightening burst ($n = 7$) to $50 R_{\odot}$ as suggested by K10. The dotted line is steepest rate of brightening burst ($n = 9$) suggested by K10.

back-scattering, and g_f and g_b are forward and back-scattering asymmetry factors. Marcus (2007) found $k = 0.95$, $g_f = 0.9$, and $g_b = -0.6$ by fitting the data to observations of six comets. For optical observations, $\delta_{90} = 1$ is used for normal and $\delta_{90} = 10$ is used for dusty comets. However, K10 suggests Kreutz comets have stronger sodium emission compared to other comets and recommends using $\delta_{90} = 0.52$ for *SOHO*'s broadband observations. For COR-2 and HI-1, as no δ_{90} have been reported, we tentatively assign $\delta_{90} = 10$ for COR-2 and $\delta_{90} = 1$ for HI-1 given that no emission lines have been found in the main transmission region of COR-2 and HI-1 using the spectrum of C/Ikeya-Seki (i.e., 630–750 nm, see Preston 1967, and many others). The δ_{90} value for HI-1 is smaller as HI-1 has the “blue leak” issue (Bewsher et al. 2010) that makes the flux contaminated by some gaseous species such as CN.

Ground-based observations are only compared with C3 observations (Figure 5), as observations from other instruments suffer from small coverage (C2 and COR-2), or blue leak contamination (HI-1).

We also note that only a subset of COR-2 data is used in this work, as all COR-2 images are polarized. Here we only use COR-2 images taken with two polarizers oriented to 0° and 90° , that can be approximated to “total brightness” images, due to the fact that cometary light is dominantly linearly polarized. Analysis of the polarized data will be reported in a separate paper.

4.3. A Note on the 2012 October Observation

No Kreutz comets with good orbits match our October observations. Our simulation shows that any comet that may position in our October images would arrive at its perihelion in 2012 November 8–15. The *SOHO* discovery catalog⁹ shows seven comets (*SOHO*-2389 to *SOHO*-2395) that reach perihelion within this time window and could have been positioned in the October images. Considering that about 95% of bright *SOHO*-observed comets move in orbits close to C/1843 D1 (Sekanina & Kracht 2013), the projected on-sky area of which is well covered in our survey, it is likely that all these seven comets ($7 \times 95\% = 6.65 \approx 7$) are within our images from a statistical perspective. Of these seven comets, three are discovered in C3 and therefore should be bright enough for our survey

should they follow K10's nominal rate. Since no comets are detected, we conclude that these comets, if they were indeed within our images, were no brighter than 21.7 mag (normalized to $\Delta = 1$ AU).

4.4. Composite light Curves of the Kreutz Family

To produce a composite set of pre-perihelion light curves of Kreutz comets, we measure two other bright Kreutz comets that emerged in recent years and that have been observed or constrained by ground-based telescopes, C/2011 W3 (Lovejoy)¹⁰ and C/2012 E2 (SWAN),¹¹ and compile our results with the results from previous studies. Ground-based observations and C3 measurements are shown as Figure 6. *STEREO* measurements are conducted following the same procedure used on C/*STEREO* and *SOHO*-2388. They are then converted to the Johnson–Cousins system following the method proposed by Bewsher et al. (2010) and modified by Hui (2013). The light curve fits of C/1965 S1 (Ikeya-Seki) and C/2011 W3 (Lovejoy) are taken from Sekanina (2002) and Sekanina & Chodas (2012). The upper limit of peak brightness of C/Lovejoy is reported by Karl Battams.¹²

We pay special attention to C/SWAN, the only Kreutz comet detected by SWAN until now. SWAN, or the Solar Wind ANisotropies camera, is an all-sky camera on board the *SOHO* spacecraft that makes daily observation of Lyman- α emission. SWAN's low spatial resolution (on the order of 1°) makes photometric calibration difficult; therefore, we use the detection limit (~ 12 mag) constrained using “gassy” comet, 2P/Encke, as the lower limit of C/SWAN in SWAN observations (a dustier comet needs to be brighter to be visible in SWAN image, potentially resulting an overestimation of the lower limit of C/SWAN's brightness). We also locate four Siding Spring Survey (SSS) images (c.f. Drake et al. 2009) taken on 2012 February 14 that cover the predicted on-sky uncertainty area of C/SWAN (of which $r_H = 1.06$ AU). We mask out the background stars and stack the images at the predicted motion rate of the comet,

¹⁰ We measure C/Lovejoy in HI-1 data until it reaches ~ 1.5 mag and saturate the detector. No COR-2 measurement can be made as the images are saturated.

¹¹ Only HI-1B and COR-2B measurements can be made. The comet was not visible in HI-1A, and COR-2A misses data taken with combined polarizers.

¹² http://sungrazer.nrl.navy.mil/index.php?p=news/birthday_comet retrieved 2014 July 30.

⁹ <https://www.ast.cam.ac.uk/~jds/knos12.htm>, retrieved 2014 July 21.

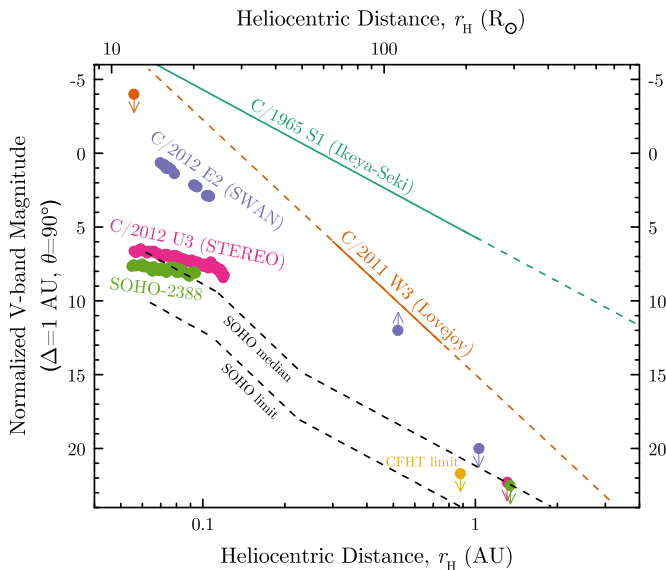


Figure 6. Composite light curves of Kreutz comets with observation up to ~ 1 AU. The brightening rate of C/1965 S1 (Ikeya-Seki) is reported by Sekanina (2002). The brightening rate of C/2011 W3 (Lovejoy) is reported by Sekanina & Chodas (2012). The solid lines are observation-based bright-curves, while dashed lines are extrapolations following the brightening rates. The light curves of C/2012 E2 (SWAN), C/2012 U3 (STEREO), and SOHO-2388 are from this work. The theoretical light curves for median (50% percentile) and faintest Kreutz comets from K10’s sample are also plotted. The brightening burst assumes a brightening rate of $n = 7$.

(A color version of this figure is available in the online journal.)

which does not show any comet down to $m_V = 20.0$ mag. We also check other bright Kreutz comets in SSS’s exposure catalog, including C/2009 Y4, C/2010 B3, C/2010 E6, C/2010 V8, and C/2010 W2, but there are no matches.

5. DISCUSSION

5.1. C/1965 S1 (Ikeya-Seki) and C/2011 W3 (Lovejoy)

C/Ikeya-Seki brightened steadily from discovery ($r_H = 1$ AU) to ~ 0.03 AU with $n = 4$. The comet was not observed from 50 to $20 R_\odot$, but the lack of offset between the two segments beside the unobserved segment of the light curve supports the idea that the comet did not deviate much from $n = 4$ in the unobserved segment.

C/Lovejoy also brightened steadily for the most part since discovery ($r_H = 0.75$ AU) but followed $n = 6.9$ (Sekanina & Chodas 2012). HI-1 observation indicates that the brightening rate gradually decreased from $n = 9.8$ to $n = 4.1$ from $r_H = 0.3$ to 0.2 AU. It is interesting to note that the brightening rate near $r_H = 0.3$ AU constrained by HI-1 is steeper than the one derived from the ground. Alternating δ_{90} would not help much to remove this discrepancy, since the observations are conducted at $\theta \sim 85^\circ$, and thus bear minimal phase angle effects. The feature could be explained by short-term fluctuations of the comet’s brightness, as hinted by the data points in Sekanina & Chodas (2012; Figure 6). Another possible cause is the relative increase of species HI-1 detectors sensitive to but not to most ground-based observers, prominently blueward species like CN (388.3 nm). Simultaneous broadband measurements would help to confirm or rule out this possibility, but unfortunately no measurements can be taken from C3 as the comet is saturated.

The fact that C/Lovejoy follows $n = 6.9$ within $r_H = 0.75$ to 0.25 AU (161 to $54 R_\odot$) seems to argue against K10’s idea that the brightening burst is unlikely to start beyond $50 R_\odot$.

Since the comet must follow $n \sim 2$ when it is far away from the Sun and behaves like an asteroid, a steep brightening rate like $n = 6.9$ must begin somewhere during the journey, presumably controlled by the dominant volatile when the comet becomes active. This would indicate that C/Lovejoy has an abundant supply of such volatiles so that it can maintain the steeper $n = 6.9$ until $r_H = 0.25$ AU. The gradual decrease to $n = 4$ also seems to indicate that the volatile is being depleted. An alternative but also plausible scenario is that C/Lovejoy underwent a series of minor outbursts that helped it to maintain a steeper brightening rate. Extending the light curve to a larger r_H would be useful to test both hypotheses, but an examination of SSS’s exposure catalog does not turn up any pre-discovery images.

No useful light curve can be obtained shortly before C/Lovejoy’s perihelion (within $r_H = 0.1$ AU) due to saturation, but we conclude that C/Lovejoy follows $n = 4$ to its peak brightness, as this agrees with the upper limit of the peak magnitude.

5.2. C/2012 E2 (SWAN)

C/SWAN is truly an exception as no other known SOHO-observed Kreutz comet—including those with peak magnitudes comparable to or brighter than C/SWAN—has been bright enough to be seen by SWAN.

SSS’s negative detection can be used to constrain the upper limit of the cometary nucleus. Assuming $A_p = 0.05$, the diameter of the nucleus can be estimated by $D = 5943 \times 10^{-H_0/5}$ with D in kilometers and H_0 is the absolute magnitude of the comet. We get $D = 680$ m as the upper limit for C/SWAN, appropriate to $r_H = 1.06$ AU. The non-detection also suggests that C/SWAN experienced an outburst with $n \gtrsim 11$ between $r_H = 1.06$ AU to 0.52 AU, then steadily followed $n = 4$ from 0.52 AU until perihelion as suggested by SWAN, C3, and HI-1 light curves. Following K10’s methodology, we estimate C/SWAN was ~ 80 m in diameter at its peak brightness.

While the light curves of SWAN, C3, and HI-1 fit well into each other, the COR-2 light curve shows a short, rapid brightening just beyond $20 R_\odot$ (Figure 7). This is puzzling as such a feature is absent in the C3 data (some C3 data are too noisy to calibrate and are therefore ignored, leaving gaps in the C3 light curve). The major cometary species in the COR-2 bandpass would be NH_2 , but previous studies of C/Ikeya-Seki (e.g., Preston 1967, and many others) showed no NH_2 emissions at $r_H = 0.1$ AU and beyond. It is unlikely that C/SWAN is different than C/Ikeya-Seki in composition and possesses some NH_2 , as they are descendants of a common parent and should be similar in composition. A more likely explanation is that since gas emission is primarily in broadband wavelengths (C3) but not in narrowband wavelengths (COR-2), a sudden decrease in gas emission would result a “shallower” increase in broadband magnitude comparing to narrowband magnitude. This probably indicates the erosion of the less volatile portion of the nucleus.

Since the transmission ranges of COR-2 and HI-1 largely overlap, the magnitude difference between these two instruments is worth some attention. The main transmission bandpasses for COR-2 and HI-1 are $650\text{--}750$ nm and $630\text{--}730$ nm, respectively, which should bear little difference as no known emission species for Kreutz comets falls in this region. The most plausible explanation is the gas contamination in the “blue leak” region, most likely CN (388.3 nm). Deriving a number for the production rate is possible but risky due to the detector’s uneven response across different wavelengths. On the other

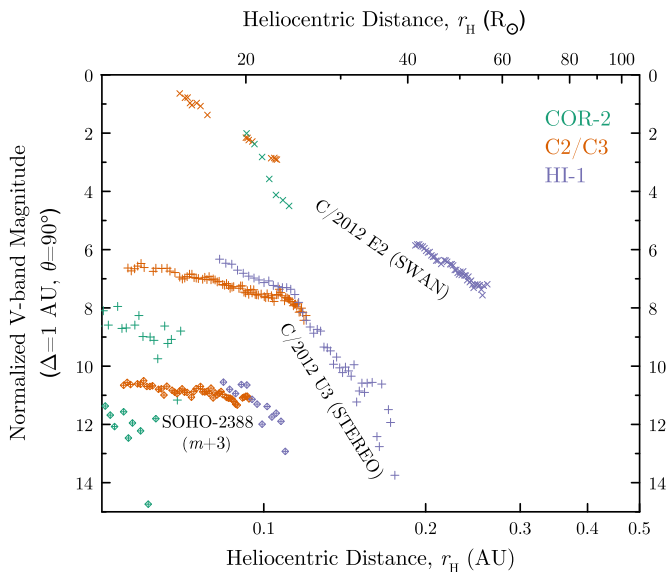


Figure 7. light curves of C/2012 E2 (SWAN), C/2012 U3 (STEREO), and SOHO-2388 (offset by 3 magnitudes for clarity) in COR-2, C2/C3, and HI-1. Different symbols represent different comets, from top to bottom or right to left: C/SWAN, C/STEREO, and SOHO-2388.

(A color version of this figure is available in the online journal.)

hand, Fe I emission (dominantly 371.9 nm and 404.5 nm) has also been reported in C/Ikeya-Seki’s post-perihelion spectrum (e.g., Preston 1967), but we doubt that Fe I can be a major contribution as the comet must be cooler at the same r_H in its pre-perihelion leg.

We also examine the water production rate of C/SWAN derived from SWAN data (Combi et al. 2013), shown in Figure 8. The water production rate of C/2012 S1 (ISON; Combi et al. 2013), a dynamically new sungrazing comet that does not belong to the Kreutz family, is also drawn for comparison. For C/SWAN, the increase of water production rate follows $n = 5.4$ from $r_H = 0.57$ to 0.36 AU after the presumed outburst. It is noteworthy that C/ISON follows a similar slope ($n = 5.3$) after an outburst as noted by ground-based observers (e.g., Ye et al. 2013), although this could well be coincidence, as we find no reason to believe that the composition and structure of the two comets is similar.

The compositional difference between C/SWAN (and its fellow Kreutz comets) and C/ISON is further suggested by the non-detection of any mini Kreutz comets by ground-based surveys. C/ISON was evidently more active at large r_H , being discovered at $m = 19$ at $r_H = 6$ AU. At the peak distance of mini Kreutz comets, C/ISON was ~ 10 mag brighter than the faintest Kreutz comet detectable by C3. Considering that C/ISON had reached $m = 10$ mag at $r_H = 1.5$ AU, if C3-detectable mini Kreutz comets are as active as C/ISON, they should have reached the detection limits of modern Near-Earth Object surveys such as the SSS (~ 20 mag) at similar r_H . The fact that no Kreutz comets at these sizes have been detected may suggest that the surface layers of mini Kreutz comets are relatively devoid of the species that drove C/ISON’s activity at large r_H such as CO_2 (Meech et al. 2013).

Using SWAN’s observations, we estimate the active area of C/SWAN to be of the order of 0.1 km^2 at $r_H = 0.5$ AU based on the vaporization model of Cowan & A’Hearn (1979). This places a lower limit of 200 m on the nucleus, which is substantially larger than the ~ 80 m value constrained by the peak brightness observed by SOHO. A similar size reduction was noted for

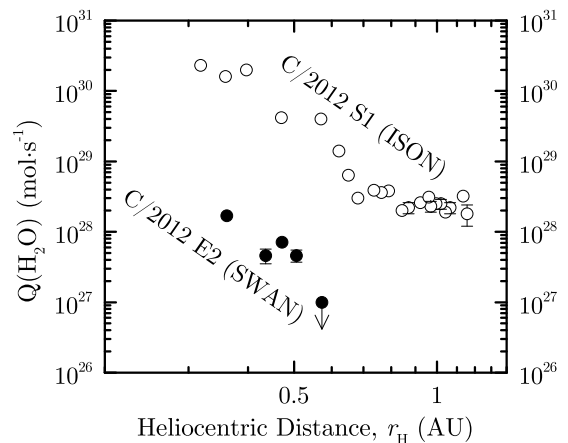


Figure 8. Water production rates of C/2012 E2 (SWAN) and C/2012 S1 (ISON) as derived by Combi et al. (2012, 2013). Some error bars are too small to appear on the figure.

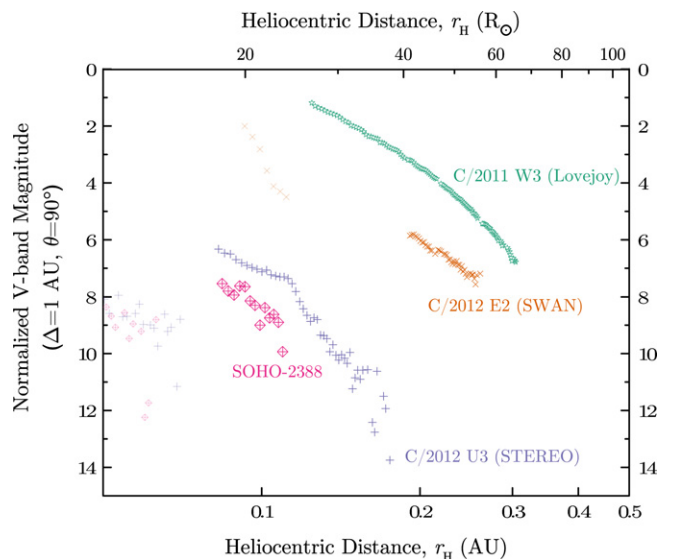


Figure 9. light curves of C/2011 W3 (Lovejoy), C/2012 E2 (SWAN), and C/2012 U3 (STEREO) derived from HI-1 data. COR-2 light curves are plotted in lighter colors. There is no COR-2 measurement for C/Lovejoy due to saturation. (A color version of this figure is available in the online journal.)

C/ISON (Knight & Battams 2014), but the reduction for C/SWAN (200 m versus 80 m) is not as large as C/ISON’s (~ 1.5 km versus ~ 100 m). While the exact numbers are probably not to be trusted, such a distinct difference suggests that C/ISON loses mass more efficiently. The fact that other bright Kreutz comets (e.g., C/Lovejoy) are undetected by SWAN may imply that C/SWAN loses mass more efficiently than its fellows, or that it contains more watery volatile than others.

5.3. C/2012 U3 (STEREO) and SOHO-2388

The non-detections by CFHT suggest upper limits of sizes of 240 m and 220 m, respectively, for C/STEREO (at $r_H = 1.31$ AU) and SOHO-2388 (at $r_H = 1.34$ AU). The non-detections indicate that C/STEREO and SOHO-2388 have $n \gtrsim 7$ during their brightening burst or their brightening bursts start beyond $50 R_\odot$. Since their light curves behave similarly to that of C/Lovejoy based on the available data, it is possible that they follow a similar pattern of C/Lovejoy and that their brightening burst stages extend to ~ 1 AU.

We also see a discrepancy in brightening rates constrained by different instruments, notably for C/*STEREO*, where $n(\text{C3}) = 7.9$, $n(\text{HI-1}) = 15.0$ near $25 R_{\odot}$, and $n(\text{C3}) = 1.8$, $n(\text{COR-2}) = 4.2$ near $15 R_{\odot}$ (Figures 7 and 9). Altering δ_{90} to extreme values (such as $\delta_{90} = 100$) produces little change and we conclude that such a discrepancy must be caused by emissions that exist in the bandpass of one instrument but not the other. Following the discussion for C/*SWAN*, the discrepancy between C3 and HI-1 is most likely due to a blueward species such as CN. We can also infer that sodium is probably not the primary driver for the brightening burst, as C3's brightening rate would benefit instead of lag if the emission is originated in the C3 bandpass (such as sodium). The discrepancy between C3 and COR-2 may have a similar nature to C/*SWAN*'s feature at $22 R_{\odot}$ and is probably due to erosion of the less-volatile portion of the nucleus.

6. CONCLUSION

We conducted a search for mini Kreutz comets at moderate heliocentric distance. Assisted by *SOHO/STEREO* observations, we identified two such comets that should be in our images but are not detected. Combining with the results from previous workers, we concluded that the brightening burst stage of these comets has $n \gtrsim 7$ or the brightening burst starts beyond $50 R_{\odot}$.

We also compiled a composite set of pre-perihelion light curves of some bright Kreutz comets that covers to ~ 1 AU, including C/1965 S1 (Ikeya-Seki), C/2011 W3 (Lovejoy), C/2012 E2 (SWAN), C/2012 U3 (*STEREO*), and *SOHO*-2388. We found at least two distinct shapes: C/Ikeya-Seki and C/*SWAN* follow $n = 4$ and others follow $n \geq 7$.

C/*SWAN* is particularly interesting, as a non-detection at $r_{\text{H}} = 1.06$ AU suggested an outburst ($\Delta m > 5$ mag) or a rapid brightening ($n \gtrsim 11$) that occur somewhere between $r_{\text{H}} = 1.06$ AU to 0.52 AU. Although broadband photometry suggested a steady brightening with $n = 4$ to perihelion, a brief surge was observed at $r_{\text{H}} = 0.1$ AU solely in the 650–750 nm range, probably hinting at the erosion of a less-volatile portion of cometary nucleus. We estimated the size of C/*SWAN*'s nucleus to be < 680 m at $r_{\text{H}} = 1.06$ AU, ~ 200 m at $r_{\text{H}} = 0.5$ AU and ~ 80 m at $r_{\text{H}} = 0.1$ AU. The reduction of nucleus size from $r_{\text{H}} = 0.5$ to 0.1 AU for C/*SWAN* is substantially smaller than that of C/2012 S1 (ISON), seemingly suggesting that C/*SWAN* loses mass less efficiently than C/ISON. The fact that other bright Kreutz comets (like C/Lovejoy) were undetected by *SWAN* may imply that C/*SWAN* either loses mass more efficiently or contains more water-ice than its compatriots. The early detection of C/ISON at large r_{H} and the non-detection of any mini Kreutz comets indicate that the surface layers of mini Kreutz comets are relatively devoid of the species that drove C/ISON's activity at large r_{H} such as CO_2 .

C/*STEREO* was concurrently observed by COR-2, C3, and HI-1; it brightened more rapidly in HI-1 than C3 at brightening burst, which suggests that a blueward species (probably CN) may be the main driver instead of sodium. C/*STEREO* also brightened faster in COR-2 than C3 at $15 R_{\odot}$, which may be similar to C/*SWAN*'s COR-2 surge in nature and is probably due to erosion of the less-volatile portion of the nucleus.

Light curve analysis is a useful tool to probe the intrinsic properties of comets. This may be especially true for comets with unique orbits like the Kreutz comets, in which the physical/chemical process are accelerated and magnified due to the extreme environment they suffer. In this study we see hints of diversity among the selected comets from light curves extended

to ~ 1 AU. Future studies aiming at determining longer segments of pre-perihelion light curves of a more statistically meaningful set of Kreutz comets may help uncover the physics behind this diversity.

We thank the anonymous referee for very thorough comments that help improve this work. We thank Karl Battams, Matthew Knight, and Joe Marcus for helpful discussions, and Jason Gill for maintaining the hardware used for data analyses. We gratefully acknowledge the CFHT operation team and *SOHO/STEREO* operation teams for their works, as well as all the *SOHO/STEREO* comet hunters for their contribution. We also thank Eric Christensen and Robert McNaught for help on the SSS data. Q.-Z. thanks Peter Brown for his encouragement and support, as well as Pauline Barmby and Reto Musci for their help on the paperwork; he also thanks Summer Xia Han for help fighting his procrastination. Parts of the observational data in this work are based on observations obtained with MegaPrime/MegaCam, a joint project of CFHT and CEA/DAPNIA, at the Canada–France–Hawaii Telescope (CFHT), which is operated by the National Research Council (NRC) of Canada, the Institut National des Science de l'Univers of the Centre National de la Recherche Scientifique (CNRS) of France, and the University of Hawaii. The SSS survey was operated by the Catalina Sky Survey (CSS) in collaboration with the Australian National University. The CSS/SSS surveys are funded by the National Aeronautics and Space Administration under grant No. NNH12ZDA001N-NEOO, issued through the Science Mission Directorate's Near Earth Object Observations Program. This work was performed in part with the support of the Natural Sciences and Engineering Research Council of Canada.

REFERENCES

- August, T. M., & Wiegert, P. A. 2013, *AJ*, **145**, 152
 Bewsher, D., Brown, D. S., Eyles, C. J., et al. 2010, *SoPh*, **264**, 433
 Combi, M. R., Bertaux, J.-L., Quemerais, E., Maekinen, J. T. T., & Ferron, S. 2013, *IACU*, **9266**, 1
 Combi, M. R., Bertaux, J.-L., Quemerais, E., Maekinen, J. T. T., & Williams, G. V. 2012, *IACU*, **9252**, 2
 Cowan, J. J., & A'Hearn, M. F. 1979, *M&P*, **21**, 155
 de Kat, J., & Abbon, P. 2000, *Proc. SPIE*, **4008**, 427
 Domingo, V., Fleck, B., & Poland, A. I. 1995, *SoPh*, **162**, 1
 Drake, A. J., Djorgovski, S. G., Mahabal, A., et al. 2009, *ApJ*, **696**, 870
 Eyles, C. J., Harrison, R. A., Davis, C. J., et al. 2009, *SoPh*, **254**, 387
 Freeland, S. L., & Handy, B. N. 1998, *SoPh*, **182**, 497
 Gilbert, A. M., & Wiegert, P. A. 2009, *Icar*, **201**, 714
 Gilbert, A. M., & Wiegert, P. A. 2010, *Icar*, **210**, 998
 Hui, M.-T. 2013, *MNRAS*, **436**, 1564
 Jordi, K., Grebel, E. K., & Ammon, K. 2006, *A&A*, **460**, 339
 Kimura, H., Mann, I., Biesecker, D. A., & Jessberger, E. K. 2002, *Icar*, **159**, 529
 Knight, M. M., A'Hearn, M. F., Biesecker, D. A., et al. 2010, *AJ*, **139**, 926
 Knight, M. M., & Battams, K. 2014, *ApJL*, **782**, L37
 Kreutz, H. C. F. 1888, Untersuchungen über das Cometensystem 1843 I, 1880 I und 1882 II, K92
 MacQueen, R. M., & St. Cyr, O. C. 1991, *Icar*, **90**, 96
 Marcus, J. N. 2007, *ICQ*, **29**, 39
 Marsden, B. G. 1967, *AJ*, **72**, 1170
 Marsden, B. G. 1989, *AJ*, **98**, 2306
 Meech, K. J., Yang, B., Kleyana, J., et al. 2013, *ApJL*, **776**, L20
 Preston, G. W. 1967, *ApJ*, **147**, 718
 Sekanina, Z. 2002, *ApJ*, **566**, 577
 Sekanina, Z., & Chodas, P. W. 2004, *ApJ*, **607**, 620
 Sekanina, Z., & Chodas, P. W. 2007, *ApJ*, **663**, 657
 Sekanina, Z., & Chodas, P. W. 2012, *ApJ*, **757**, 127
 Sekanina, Z., & Kracht, R. 2013, *ApJ*, **778**, 24
 Wiegert, P., Balam, D., Moss, A., et al. 2007, *AJ*, **133**, 1609
 Ye, Q. Z., Hui, M. T., & Gao, X. 2013, *CBET*, **3718**, 2
 Zacharias, N., Monet, D. G., Levine, S. E., et al. 2004, *BAAS*, **36**, 1418